

**EFFECT OF VORTICITY COHERENCE ON
ENERGY-ENSTROPY BOUNDS FOR THE 3D
NAVIER-STOKES EQUATIONS**

R. DASCALIUC¹, Z. GRUJIĆ², AND M. S. JOLLY³

ABSTRACT. Bounding curves in the energy, enstrophy-plane are derived for the 3D Navier-Stokes equations under an assumption on coherence of the vorticity direction. The analysis in the critical case where the direction is Hölder continuous with exponent $r = 1/2$ results in a curve with extraordinarily large maximal enstrophy (exponential in Grashof), in marked contrast to the sub-critical case, $r > 1/2$ (algebraic in Grashof).

Dedicated to Ciprian Foias in appreciation of his unbounded generosity

1. INTRODUCTION

Numerical simulations of turbulent flows (cf. [1, 21, 27, 31]) reveal regions of *intense vorticity* dominated by coherent vortex structures; more specifically, *vortex filaments*. One of the imminent morphological signatures of the filamentary geometry is the *local coherence of the vorticity direction*; it turns out that this property of turbulent flows leads to the *geometric depletion of the nonlinearity*.

The pioneering work in this direction was made by Constantin. He obtained in [8] a singular integral representation of the stretching factor in the evolution of the vorticity magnitude featuring a geometric kernel that is depleted by local coherence of the vorticity direction, a purely geometric condition. This led to the first rigorous confirmation in [9] of the local anisotropic dissipation in the 3D NSE: a theorem stating that as long as the vorticity direction is Lipschitz-coherent (in the regions of high vorticity), the L^2 -norm of the vorticity is controlled, and no finite time blow-up can occur.

Subsequent work delved further into this geometric condition. The relaxation of the Lipschitz-coherence condition to a $\frac{1}{2}$ -Hölder condition was made in [3], followed by a full *spatiotemporal localization* of the $\frac{1}{2}$ -Hölder condition in [19]. A family of local, hybrid, geometric-analytic regularity criteria including a *scaling invariant* improvement of the $\frac{1}{2}$ -Hölder condition was presented in [20]. Studies of coherence of the vorticity direction-type regularity criteria on bounded domains in the cases of no-stress and no-slip boundary conditions were presented in [4] and [2], respectively.

Date: September 30, 2018.

2000 Mathematics Subject Classification. 35Q30, 76F02.

Key words and phrases. Navier-Stokes equations, turbulence.

R.D. was supported in part by National Science Foundation grant DMS-1211413. Z.G. acknowledges support of the Research Council of Norway via grant 213474/F20, and the NSF via grant DMS 1212023. M.S.J. was supported in part by NSF grant numbers DMS -1008661 and DMS-1109638.

In this paper we derive a bounding curve for the weak attractor in the plane spanned by energy e and enstrophy \mathcal{E} under the $\frac{1}{2}$ -Hölder condition in [3]. These curves suggest two scenarios in which the Taylor wave number κ_T can satisfy

$$(1.1) \quad \kappa_T := \left(\frac{\langle \mathcal{E} \rangle}{\langle e \rangle} \right)^{1/2} \gg \bar{\kappa}$$

where $\bar{\kappa}$ is the largest wavenumber in the force. One is where both energy and enstrophy are small; the other is where there are brief, intense bursts of large enstrophy. It is shown in [17, 16] that (1.1) guarantees the energy cascade predicted by the Kolmogorov theory of turbulence [22]. The $\frac{1}{2}$ -Hölder condition is essential for our analysis, of course. Yet, if the resulting curve turns out to be sharp, this condition still allows for excursions with extraordinarily large enstrophy; the maximum value achieved by this curve is $\mathcal{E}_{\max} = \mathcal{O}(\exp(G^2))$, where G is the Grashof number. This would mean that if the $\frac{1}{2}$ -Hölder condition were valid, solutions that are in fact regular might appear to blow-up in finite time under numerical simulation.

The approach for the bounding curves follows that of Foias and Prodi (see pages 59-61 in [14] as well as [15, 11]). Each curve solves an ordinary differential equation in which e , \mathcal{E} are the independent and dependent variables respectively. The ODE is formed by the quotient of estimates for the growth rates de/dt and $d\mathcal{E}/dt$ in a region of the e , \mathcal{E} -plane where $de/dt < 0$. This technique was applied to the 2D NSE in both the energy, enstrophy-plane in [11], as well as in the enstrophy, palinstrophy-plane in [12], the latter being more relevant to the Kraichnan theory of 2D turbulence [23]. Curves which close were also found in this manner in [13] for the 3D Leray- α and the 3D Navier-Stokes- α models, whose solutions are global in time and approach those of the 3D NSE as the filter width parameter $\alpha \rightarrow 0$ [7, 32]. As expected, however, these bounding curves for the α -models blow up as $\alpha \rightarrow 0$.

For comparison, we include in this paper curves that somewhat limit solutions for the full NSE, i.e., without any conditions. Of course, using current techniques for estimating growth rates, those curves do not close. In [26] Doering uses the system of differential inequalities given by growth rate estimates to show that for initial data satisfying $\mathcal{E}_0 \lesssim \nu^4/e_0$ the enstrophy remains bounded. The maximal enstrophy growth rate for given enstrophy was studied numerically in [25].

In order to properly assess the significance of the $\frac{1}{2}$ -Hölder condition in the realm of dynamics within the energy, enstrophy-plane, we also include the results describing the effects of the sub-critical coherence case where the Hölder exponent satisfies $1/2 < r \leq 1$, as well as the effects of an example of the more traditional scaling-invariant conditions on the vorticity magnitude, namely, the small, uniform-in-time, $L^{\frac{3}{2}}$ -spatial integrability condition. It is worth observing that there is a *qualitative jump* between the maximal enstrophy allowed in the sub-critical and in the $\frac{1}{2}$ -Hölder coherence scenarios; more precisely, from algebraic in G to exponential in G . Perhaps more intriguing is the comparison between the whole range of the Hölder coherence conditions and the $L^{\frac{3}{2}}$ -condition. With respect to the scaling inherent to the 3D NSE, the $L^{\frac{3}{2}}$ -condition is scaling invariant, and the Hölder coherence conditions are all sub-critical; hence—in this metric—the $L^{\frac{3}{2}}$ -condition is a weaker condition. In contrast, the $L^{\frac{3}{2}}$ -condition produces the most restrictive maximal curve in the energy, enstrophy-plane, and is—in this sense—a *dynamically stronger condition*.

After some preliminaries in Section 2, we derive the bounding curves for the full NSE in Section 3. The precise formulation of the Hölder condition is given in Section 4. The critical case, Hölder exponent $r = 1/2$, is treated in Section 5 resulting in a bounding curve in terms of incomplete gamma functions, followed by sharp estimates for the maximum enstrophy value for this curve. Section 7 and Section 8 address the sub-critical Hölder coherence and the scaling-invariant $L^{\frac{3}{2}}$ -spatial integrability cases, respectively.

2. PRELIMINARIES

We consider the incompressible Navier-Stokes equations (NSE) in a bounded, connected, open set $\Omega \in \mathbb{R}^3$

$$(2.1) \quad \frac{\partial u}{\partial t} - \nu \Delta u + (u \cdot \nabla)u + \nabla p = F, \quad x \in \Omega$$

$$(2.2) \quad \nabla \cdot v = 0,$$

with either periodic or no-slip boundary conditions. The NSE can be written in functional form as

$$(2.3) \quad \frac{du}{dt} + \nu Au + B(u, u) = f, \quad u \in H$$

where H is an appropriate (L^2 -based) Hilbert space, $A = -P\Delta$ is the Stokes operator, $B(u, v) = P(u \cdot \nabla)v$, $f = PF$, and P is the Helmholtz-Leray projector onto divergence-free functions. In this case, A is a positive definite self-adjoint operator with compact inverse, and we will denote by $\lambda(> 0)$ its smallest eigenvalue. To measure the size of the body force f , we introduce the dimensionless Grashof number

$$G = \frac{\|f\|_2}{\nu^2 \lambda^{3/4}},$$

where $\|\cdot\|_2$ is the L^2 -norm on Ω . A more detailed description of this functional setting for the NSE can be found in [30].

One of the main results of the (yet incomplete) NSE regularity theory is the existence of *Leray-Hopf weak solutions* to the initial value problem associated with (2.3). For an arbitrary $T > 0$ (fixed), any Leray-Hopf solution is $\mathcal{D}(A)$ -valued except, possibly, on a closed subset of $[0, T]$ of $1/2$ -dimensional Hausdorff measure 0. Thus it is regular on an open set which can then be written in the worst case as a union of countably many mutually disjoint open intervals, a set that is dense in $[0, \infty)$. See [10], [24], and [29] for general background on the regularity theory of the NSE.

We will use several well-known properties of the nonlinear term B , namely

$$(2.4) \quad B(u, v, v) = 0, \quad \forall u \in H, v \in V = \mathcal{D}(A^{1/2})$$

and

$$(2.5) \quad |(B(u, u), Au)| \leq c \|A^{1/2}u\|_2^{3/2} \|Au\|_2^{3/2},$$

(see (6.18) and (9.22) in [10]). Throughout the paper c will denote a generic, dimensionless constant, which will change from line to line, except when distinguished by a subscript.

Within each interval of regularity, we can take the L^2 -scalar product of (2.3) with u , and then applying (2.4), the Cauchy-Schwarz and Young inequalities, one has the standard differential relation for energy

$$(2.6) \quad \frac{d\|u\|_2^2}{dt} + 2\nu\|A^{1/2}u\|_2^2 \leq 2\|f\|_2\|u\|_2 = 2\nu^2\lambda^{3/4}Ge^{1/2} \leq \nu^3\lambda^{1/2}G^2 + \nu\lambda\|u\|_2^2,$$

which, together with the Poincaré and Gronwall inequalities, implies that for regular solutions

$$\limsup_{t \rightarrow \infty} \|u\|_2^2 \leq \frac{\|f\|_2^2}{\nu^2\lambda^2} = \frac{\nu^2G^2}{\lambda^{1/2}}.$$

In fact this property holds for general Leray-Hopf solutions.

More precisely, the long-time behavior of (2.3) is encoded in the weak attractor, \mathcal{A}_w (first introduced in [18]), the subset of Leray-Hopf solutions that are globally bounded in H – forward and backward in time. This set weakly attracts all Leray-Hopf solutions as $t \rightarrow \infty$. By using the Leray-Hopf energy inequality one can establish that \mathcal{A}_w is contained in a ball in H centered at 0 with radius $\nu G/\lambda^{1/4}$, i.e.,

$$(2.7) \quad \mathcal{A}_w \subseteq B(0, \nu G/\lambda^{1/4}).$$

In particular $B(0, \nu G/\lambda^{1/4})$, is a (forward in time) invariant set for the Leray-Hopf solutions. Therefore, in what follows our study of energy-entropy relations will be focused *exclusively on this ball*.

We conclude by noting that the above theory of Leray-Hopf solutions will be less relevant in the no-slip case studied in Sections 5-7, since the vorticity coherence assumption (4.4) combined with (5.1) imply that the solution is in fact regular, and therefore estimates like (2.6) will hold for all t .

3. BOUNDS FOR THE FULL 3D NAVIER-STOKES EQUATIONS

While an overall bound on enstrophy for the 3D NSE remains an open question, the partial regularity results described above will allow us to derive certain curves in the energy, enstrophy-plane which limit the long time behavior of Leray-Hopf solutions, without any additional regularity assumptions.

In this section we consider periodic boundary conditions on $\Omega = [0, L]^3$, take the phase space H for (2.3) to be the closure in $L^2(\Omega)^3$ of all divergence-free, mean zero trigonometric polynomials, and denote the energy, enstrophy and palinstrophy by

$$e = \|u\|_2^2, \quad E = \|A^{1/2}u\|_2^2, \quad P = \|Au\|_2^2.$$

As noted before, we will concentrate on the globally bounded solutions, for which (2.7) holds, i.e:

$$(3.1) \quad e \leq e_0 = \frac{\|f\|_2^2}{\nu^2\lambda^2} = \frac{\nu^2G^2}{\lambda^{1/2}}.$$

Now on each interval of regularity, take the L^2 -scalar product of (2.3) with Au , apply (2.5), and then proceed as in (2.6) to find

$$\begin{aligned} \frac{1}{2} \frac{dE}{dt} + \nu P &= \|f\|_2 P^{1/2} + cE^{3/4}P^{3/4} \\ &\leq \frac{\|f\|_2^2}{\nu} + \frac{\nu P}{4} + \frac{cE^3}{\nu^3} + \frac{\nu P}{4}. \end{aligned}$$

Again by the Cauchy-Schwarz inequality we have $\mathbf{E}^2 \leq \mathbf{eP}$, so that

$$(3.2) \quad \begin{aligned} \frac{d\mathbf{E}}{dt} &\leq 2\nu^3\lambda^{3/2}G^2 + \frac{c_1\mathbf{E}^3}{\nu^3} - \nu\mathbf{P} \\ &\leq 2\nu^3\lambda^{3/2}G^2 + \frac{c_1\mathbf{E}^3}{\nu^3} - \nu\frac{\mathbf{E}^2}{\mathbf{e}}. \end{aligned}$$

Note that $d\mathbf{E}/dt \leq 0$ provided

$$(3.3) \quad \mathbf{e} \leq \Psi(\mathbf{E}) = \frac{\nu^4\mathbf{E}^2}{2\nu^6\lambda^{3/2}G^2 + c_1\mathbf{E}^3},$$

and that the nonzero critical number for Φ is

$$(3.4) \quad \mathbf{E}_1 = \left(\frac{4}{c_1}\right)^{1/3} \nu^2\lambda^{1/2}G^{2/3}.$$

For some $\eta > 1$ consider the region where we have both

$$(3.5) \quad \mathbf{E} \geq \eta\nu\lambda^{3/4}G\mathbf{e}^{1/2}$$

and

$$\frac{c_1\mathbf{E}^3}{\nu^3} \geq 2\nu^3\lambda^{3/2}G^2,$$

or equivalently

$$(3.6) \quad \mathbf{E} \geq \underline{\mathbf{E}} = \left(\frac{2}{c_1}\right)^{1/3} \nu^2\lambda^{1/2}G^{2/3} = 2^{-1/3}\mathbf{E}_1.$$

Using (3.5) and (3.6) in (3.2), we have

$$(3.7) \quad \frac{d\mathbf{E}}{dt} \leq 2c_1\nu^{-3}\mathbf{E}^3 - \eta\nu^2\lambda^{3/4}G\mathbf{e}^{-1/2}\mathbf{E} \quad \text{a.e. } t \in [0, \infty),$$

while (3.5) in (2.6) gives

$$(3.8) \quad \frac{d\mathbf{e}}{dt} \leq -2(\eta - 1)\nu^2\lambda^{3/4}G\mathbf{e}^{1/2} \quad \text{a.e. } t \in [0, \infty).$$

To find a bounding curve we proceed as in [14, 15, 11]. It is constructed as a solution to an ODE in the variables \mathbf{e} , \mathbf{E} , in decreasing \mathbf{e} . As long as (3.5) holds so that the upper bound (3.8) is not positive, and as long as the bound in right hand side of (3.7) is nonnegative, the slope of this curve is determined by quotient of the two bounds. The bounding curve is then the solution to the Bernoulli ODE

$$(3.9) \quad \begin{aligned} \frac{d\mathbf{E}}{d\mathbf{e}} &= \frac{2c_1\nu^{-3}\mathbf{E}^3 - \eta\nu^2\lambda^{3/4}G\mathbf{e}^{-1/2}\mathbf{E}}{-2(\eta - 1)\nu^2\lambda^{3/4}G\mathbf{e}^{1/2}} \\ &= \frac{1}{2} \frac{\eta}{\eta - 1} \frac{\mathbf{E}}{\mathbf{e}} - \left[\frac{c_1}{(\eta - 1)\nu^5\lambda^{3/4}G} \right] \frac{\mathbf{E}^3}{\mathbf{e}^{1/2}}, \end{aligned}$$

whose solution can be written as

$$(3.10) \quad \mathbf{E} = \Phi(\mathbf{e}) = \left\{ \left(\frac{\mathbf{e}_0}{\mathbf{e}}\right)^\alpha \mathbf{E}_0^{-2} + \beta \left(\mathbf{e}^{1/2} - \mathbf{e}^{-\alpha}\mathbf{e}_0^{1/2+\alpha}\right) \right\}^{-1/2},$$

where

$$\alpha = \frac{\eta}{\eta - 1} \quad \text{and} \quad \beta = \frac{4c_1}{(3\eta - 1)\nu^5\lambda^{3/4}G}.$$

The function Φ has a vertical asymptote at $\mathbf{e} = \mathbf{e}_*$, where

$$\mathbf{e}_*^{\alpha+1/2} = \mathbf{e}_0^{\alpha+1/2} - \frac{\mathbf{e}_0^\alpha}{\beta \mathbf{E}_0^2}.$$

We assume that (3.6) holds for initial data $(\mathbf{e}_0, \mathbf{E}_0)$ on the parabola

$$(3.11) \quad \mathbf{E} = \eta \nu \lambda^{3/4} G \mathbf{e}^{1/2},$$

so that in terms of η , this asymptote is at

$$\mathbf{e}_*(\eta) = \mathbf{e}_0 \left(1 - \frac{3\eta - 1}{4c_1 \eta^2 G^4} \right)^{\frac{2(\eta-1)}{3\eta-1}}.$$

We next solve (3.9) with initial data $(\mathbf{e}_1, \mathbf{E}_1)$ given by the maximum of Ψ in (3.3), where \mathbf{E}_1 is as in (3.4) and

$$\mathbf{e}_1 = \frac{1}{6} \left(\frac{4}{c_1} \right)^{2/3} \nu^2 \lambda^{-1/2} G^{-2/3}.$$

The solution curve with this initial data would intersect the parabola (3.11) at the value of \mathbf{e} satisfying

$$(3.12) \quad \mathbf{e}^{1/2+\alpha} - \gamma \mathbf{e}^{\alpha-1} + \delta = 0$$

where

$$\gamma = \frac{1}{\beta \eta^2 \nu^2 \lambda^{3/2} G^2} \quad \text{and} \quad \delta = \frac{\mathbf{e}_1^\alpha}{\beta \mathbf{E}_1^2} - \mathbf{e}_1^{1/2+\alpha}.$$

Substituting the values for $\mathbf{e}_1, \mathbf{E}_1$, one can show that $\delta > 0$ provided

$$\eta < 1 + \frac{4c_1}{3\sqrt{6}} \left(\frac{4}{c_1} \right)^{5/6}.$$

Dropping the γ -term in (3.12), we obtain as a lower bound for its root

$$\mathbf{e}_2 > \delta^{\frac{2}{2\alpha+1}} \nu^2 \lambda^{-1/2} G^{2/3}.$$

For large G , we then have that $\mathbf{e}_2 > \underline{\mathbf{e}}$, where $(\underline{\mathbf{e}}, \underline{\mathbf{E}})$ is the point of intersection of the line $\mathbf{E} = \underline{\mathbf{E}}$ and the parabola in (3.11). A qualitative sketch of the shaded region in which the weak attractor must lie is given in Figure 1. It is not surprising that this region is not closed, since global regularity is still an open question. As far as these estimates show, the sufficient condition (large κ_T , see (1.1)) for an energy cascade can be met either by the solution spending most of its time near zero, or with repeated excursions into the intermittent region.

4. VORTEX STRETCHING DEPLETION

We now show how a geometric condition of the direction of vorticity allows us to close the region for the weak attractor. For convenience in the analysis to follow, we now consider no-slip boundary conditions

$$(4.1) \quad u(x) = 0, \quad x \in \Gamma = \partial\Omega.$$

Taking the curl of (2.1) gives the equation for the vorticity $\omega = \text{curl } u$

$$(4.2) \quad \frac{\partial \omega}{\partial t} - \nu \Delta \omega + (u \cdot \nabla) \omega = (\omega \cdot \nabla) u + \text{curl } F, \quad x \in \Omega$$

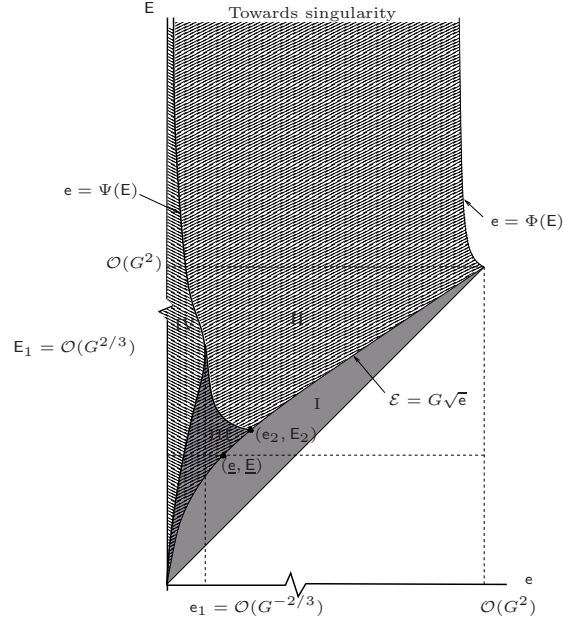


FIGURE 1. Bounds for the full 3D NSE. Region I is recurrent. If the solution blows up, it must enter region II. If it enters regions III, IV it must enter region I. In region IV the enstrophy is always decreasing, while in regions II, III, IV, the energy is always decreasing.

The evolution of the enstrophy is found by taking the scalar product of (4.2) with ω in $L^2(\Omega)$

$$(4.3) \quad \frac{1}{2} \frac{d}{dt} \|\omega\|_2^2 + \nu \|\nabla \omega\|_2^2 - \nu \int_{\Gamma} \frac{\partial \omega}{\partial n} \cdot \omega \, d\Gamma = ((\omega \cdot \nabla)u, \omega) + (\text{curl } F, \omega).$$

The obstacle to proving global existence of solutions is the vortex stretching term $((\omega \cdot \nabla)u, \omega)$. One way to mitigate its effect is to impose a geometric condition on it in physical space.

This amounts to a coherence assumption on the direction of the vorticity of the form

$$(4.4) \quad |\sin \theta(\omega(x), \omega(y))| \leq c\lambda^{r/2} |x - y|^r$$

where θ is the angle between the two vectors, and $|\cdot|$ denotes either $\|\cdot\|_{\mathbb{R}^3}$, or absolute value.

5. THE CRITICAL CASE

Following the work of Constantin and Fefferman in [9, 8], H. Beirão da Veiga shows in [2] that condition (4.4) with $r = 1/2$, along with the additional assumption

$$(5.1) \quad \int_{\Gamma} \frac{\partial \omega}{\partial n} \cdot \omega \, d\Gamma \leq \delta \|\nabla \omega\|_2^2 + \lambda \psi(t) \|\omega\|_2^2$$

for some constant $\delta < 1$ and some $\psi \in L^1(0, T)$, is sufficient for regularity of the solution to the NSE on the interval $[0, T]$. To do so he splits the vorticity as

$$\omega(x) = \omega^{(1)}(x) + \omega^{(2)}(x) = \begin{cases} \omega^{(1)}(x) & \text{if } |\omega(x)| \leq \mu\lambda\nu \\ \omega^{(2)}(x) & \text{if } |\omega(x)| > \mu\lambda\nu \end{cases}$$

for some $\mu > 0$. This leads to an expansion of the trilinear term into eight summands:

$$\begin{aligned} ((\omega \cdot \nabla)u \cdot \omega)(x) &= \sum_{\alpha, \beta, \gamma=1}^2 \mathcal{K}_{\alpha\beta\gamma}(x) \\ &= - \sum_{\alpha, \beta, \gamma=1}^2 \epsilon_{jkl} \omega_i^{(\alpha)}(x) \omega_j^{(\beta)}(x) \int_{\Omega} \frac{\partial^2 \mathcal{G}(x, y)}{\partial y_k \partial x_i} \omega_l^{(\gamma)}(y) dy \end{aligned}$$

where

$$\epsilon_{jkl} = \begin{cases} 1 & (i, j, k) \text{ even permutation} \\ -1 & (i, j, k) \text{ odd permutation} \\ 0 & i, j, k \text{ all equal} \end{cases}, \quad \text{and} \quad \mathcal{G}(x, y) = \frac{1}{4\pi|x-y|} + g(x, y)$$

for some regular function g . The only summand that uses (4.4) is \mathcal{K}_{222} . Since we will modify slightly Beirão da Veiga's estimate, we recall part of his argument. First he shows that

$$|\mathcal{K}_{222}(x)| \leq c \int_{\Omega} \frac{|\omega^{(2)}(x)|^2 |\omega^{(2)}(y)|}{|x-y|^3} |\sin \theta(x, y)| dy.$$

Then, writing I for the Riesz potential

$$I(x) = \int_{\Omega} |\omega(y)| \frac{dy}{|x-y|^{5/2}},$$

using (4.4) with $r = 1/2$, and Hölder's inequality, he finds that

$$(5.2) \quad \int_{\Omega} |\mathcal{K}_{222}(x)| dx \leq c\lambda^{1/4} \int_{\Omega} |\omega(x)|^2 I(x) dx \leq c\lambda^{1/4} \|\omega\|_2 \|\omega\|_6 \|I\|_3$$

As in [2], we apply the Hardy-Littlewood-Sobolev inequality [28] $\|I\|_3 \leq c\|\omega\|_2$ and the Sobolev embedding $H_0^1(\Omega) \subset L^6(\Omega)$, but then use the Poincaré inequality before applying Young's inequality

$$\begin{aligned} (5.3) \quad \int_{\Omega} |\mathcal{K}_{222}(x)| dx &\leq c\lambda^{1/4} \|\omega\|_2 (\lambda^{1/2} \|\omega\|_2 + \|\nabla\omega\|_2) \|\omega\|_2 \\ &\leq c\lambda^{1/4} \|\nabla\omega\|_2 \|\omega\|_2^2 \\ &\leq \varepsilon\nu \|\nabla\omega\|_2^2 + c\lambda^{1/2} \frac{\|\omega\|_2^4}{\varepsilon\nu}. \end{aligned}$$

Otherwise, except for the inclusion of dimensional factors involving ν and λ , we treat the bounds for the remaining summands as in [2]. They amount to the three cases

$$\left| \int_{\Omega} \mathcal{K}_{\alpha\beta 2}(x) dx \right| \leq c\mu\nu\lambda \|\omega\|_2^2, \quad \text{for } (\alpha, \beta) \neq (2, 2)$$

and the remaining four

$$\left| \int_{\Omega} \mathcal{K}_{\alpha\beta 1}(x) dx \right| \leq \varepsilon \nu \|\nabla \omega\|_2^2 + c\varepsilon^{-3/5}(\mu\lambda)^{4/5}\nu^{1/5}\|\omega\|_2^{4/5}\|\omega\|_2^2.$$

For the remainder of the paper we take $\mathcal{E} = \|\omega\|_2^2$ and $\mathcal{P} = \|\nabla \omega\|_2^2$ as enstrophy and palinstrophy respectively. Assuming that (4.4), (5.1) hold, we then have that

$$(5.4) \quad \frac{1}{2} \frac{d\mathcal{E}}{dt} + \nu \mathcal{P} \leq (2\varepsilon + \delta)\nu \mathcal{P} + c_2 \left[\nu\lambda(\mu + \psi) + \frac{\nu^{1/5}}{\varepsilon^{3/5}}(\mu\lambda)^{4/5}\mathcal{E}^{2/5} + \frac{\lambda^{1/2}}{\varepsilon\nu}\mathcal{E} \right] \mathcal{E} + \|\operatorname{curl} F\|_2 \mathcal{E}^{1/2}.$$

The point in applying the Poincaré inequality in (5.3) is that otherwise the summand $\lambda^{3/4}\mathcal{E}^{1/2}$ would appear in the brackets. To further simplify, we note that the summand involving $\mathcal{E}^{2/5}$ will dominate both the first summand in brackets as well as the term from the force provided

$$(5.5) \quad \mathcal{E} \geq \mathcal{E}_{\min} = \max \left\{ \frac{\varepsilon^{3/2}\lambda^{1/2}\nu^2}{\mu^2}(\mu + \|\psi\|_{\infty})^{5/2}, \frac{\varepsilon^{2/3}}{c_2^{10/9}(\mu\lambda)^{8/9}\nu^{2/9}} \|\operatorname{curl} F\|_2^{10/9} \right\},$$

where we have tacitly assumed that $\psi \in L^{\infty}(0, T)$. Now choose ε small enough to satisfy

$$(5.6) \quad 2\varepsilon + \delta = \rho < 1; .$$

Note that

$$\begin{aligned} \mathcal{E} &= \|\omega\|_2^2 \leq 2\|A^{1/2}u\|_2^2 \leq 2\|u\|_2\|Au\|_2 = 2\|u\|_2\|\Delta u\|_2 \\ &= 2\|u\|_2\|\operatorname{curl} \omega\|_2 \leq 2\|u\|_2\sqrt{2}\|\nabla \omega\|_2 = 2^{3/2}e^{1/2}\mathcal{P}^{1/2} \end{aligned}$$

hence

$$(5.7) \quad -8\mathcal{P} \leq -\mathcal{E}^2/e.$$

Gathering terms, we find that

$$(5.8) \quad \frac{d\mathcal{E}}{dt} \leq \left(\frac{c_2\lambda^{1/2}}{\varepsilon\nu} - \frac{\nu(1-\rho)}{4e} \right) \mathcal{E}^2 + \frac{6c_2(\mu\lambda)^{4/5}\nu^{1/5}}{\varepsilon^{3/5}} \mathcal{E}^{7/5}.$$

We now assume, in addition to (5.6), that

$$(5.9) \quad \nu\mathcal{E} \geq 4\|f\|_2 e^{1/2}.$$

Using this in (2.6), along with $\mathcal{E} \leq 2\|A^{1/2}u\|_2^2$ we find that

$$(5.10) \quad \frac{de}{dt} \leq -\frac{\nu}{2}\mathcal{E}.$$

As in Section 3, we assume (2.7) holds, and so, by combining (5.10) with (5.8) as indicated in Figure 2(a) we can construct a bounding curve for \mathcal{A}_w by solving

$$(5.11) \quad \frac{d\mathcal{E}}{de} = \left(\frac{1-\rho}{2e} - \frac{2c_2\lambda^{1/2}}{\varepsilon\nu^2} \right) \mathcal{E} - \frac{12c_2(\mu\lambda)^{4/5}}{\varepsilon^{3/5}\nu^{4/5}} \mathcal{E}^{2/5}$$

$$(5.12) \quad \mathcal{E}(e_0) = \mathcal{E}_0, \quad \text{where } e_0 := \frac{\nu^2 G^2}{\lambda^{1/2}} \quad \text{and}$$

$$(5.13) \quad \mathcal{E}_0 := \max \left\{ 4\|f\|_2 e_0^{1/2}, \mathcal{E}_{\min} \right\} = \max \left\{ 4\nu^2\lambda^{1/2}G^2, \mathcal{E}_{\min} \right\}$$

provided the right hand side in (5.8) is nonnegative, i.e, $(\mathbf{e}, \mathcal{E})$ is to the right of the curve

$$(5.14) \quad \mathcal{E} = \varepsilon^{2/3} \mu^{4/3} \lambda^{1/2} \nu^2 \left[\frac{6\mathbf{e}}{\mathbf{e}_a - \mathbf{e}} \right]^{5/3}, \quad \mathbf{e} < \mathbf{e}_a = \frac{\varepsilon(1-\rho)}{4c_2} \frac{\nu^2}{\lambda^{1/2}}.$$

Notice that if G is big enough, $\mathbf{e}_0 = \nu G^2 / \lambda^{1/2} > \mathbf{e}_a$, and so the solution $\mathcal{E} = \varphi_1(\mathbf{e})$ to (5.11-5.12) is indeed to the right of the curve in (5.14) over an interval $(\mathbf{e}_{\max}, \mathbf{e}_0]$. In fact, φ_1 is a decreasing curve on $[\mathbf{e}_{\max}, \mathbf{e}_0]$ with global maximum at $(\mathbf{e}_{\max}, \mathcal{E}_{\max})$ – the intersection with the curve in (5.14).

Recognizing (5.11) as a Bernoulli equation, we set

$$\xi = \mathcal{E}^{3/5}, \quad a = \frac{3(1-\rho)}{10}, \quad b = \frac{6c_2\lambda^{1/2}}{5\varepsilon\nu^2}, \quad \text{and } C = \frac{36c_2(\mu\lambda)^{4/5}}{5\varepsilon^{3/5}\nu^{4/5}}$$

to obtain

$$(5.15) \quad \frac{d\xi}{d\mathbf{e}} + \left(-\frac{a}{\mathbf{e}} + b \right) \xi = -C, \quad \xi(\mathbf{e}_0) = \xi_0 = (2\nu^3\lambda^{1/2}G^2)^{3/5}.$$

whose solution is

$$(5.16) \quad \xi(\mathbf{e}) = \mathbf{e}^a e^{-b\mathbf{e}} \left[\mathbf{e}_0^{-a} e^{b\mathbf{e}_0} \xi_0 - C \int_{\mathbf{e}_0}^{\mathbf{e}} s^{-a} e^{bs} ds \right],$$

To evaluate the integral we use an expansion of the incomplete gamma function

$$(5.17) \quad \gamma(\alpha, z) = \int_0^z \tau^{\alpha-1} e^{-\tau} d\tau = z^\alpha \sum_{n=0}^{\infty} \frac{(-z)^n}{n!(\alpha+n)},$$

so that with $\alpha = 1 - a$

$$\begin{aligned} \int_{\mathbf{e}_0}^{\mathbf{e}} s^{-a} e^{bs} ds &= (-b)^{a-1} \int_{-b\mathbf{e}_0}^{-b\mathbf{e}} \tau^{-a} e^{-\tau} d\tau \\ &= (-b)^{-\alpha} [\gamma(\alpha, -b\mathbf{e}) - \gamma(\alpha, -b\mathbf{e}_0)]. \end{aligned}$$

The solution to (5.11) can thus be written as

$$\mathcal{E} = \varphi_1(\mathbf{e}) = \left\{ \mathbf{e}^a e^{-b\mathbf{e}} \left[\mathbf{e}_0^{-a} e^{b\mathbf{e}_0} \xi_0 - C \left(\mathbf{e}^\alpha \sum_{n=0}^{\infty} \frac{(b\mathbf{e})^n}{n!(\alpha+n)} - \mathbf{e}_0^\alpha \sum_{n=0}^{\infty} \frac{(b\mathbf{e}_0)^n}{n!(\alpha+n)} \right) \right] \right\}^{5/3}.$$

To find a bounding curve for $\mathbf{e} < \mathbf{e}_{\max}$ under the assumptions (5.5) and (5.9), observe that since the right hand side in (5.8) is negative, we need a lower bound on $d\mathbf{e}/dt$. From Theorem 1.1 in [6] (henceforth, Ω is convex) there exists a constant $c_\Omega \geq 1$ depending on the domain, such that $\mathbf{E} \leq c_\Omega \mathcal{E}$. Using this in

$$-2\|f\|_2 \|u\|_2 \leq \frac{d\|u\|_2^2}{dt} + 2\nu \|A^{1/2}u\|_2^2 \leq \frac{d\mathbf{e}}{dt} + 2\nu c_\Omega \mathcal{E},$$

together with (5.9), we may now write

$$(5.18) \quad -C_\Omega \frac{\nu}{2} \mathcal{E} \leq \frac{d\mathbf{e}}{dt}, \quad C_\Omega = 1 + 4c_\Omega,$$

and combine with (5.8) to arrive at an initial-value problem similar to (5.11-5.12), but with the right-hand side of (5.11) divided by C_Ω , and the initial condition

$$\mathcal{E}(\mathbf{e}_{\max}) = \mathcal{E}_{\max} := \varphi_1(\mathbf{e}_{\max}).$$

Consequently we obtain a bounding curve $\mathcal{E} = \varphi_2(\mathbf{e}) = \xi^{5/3}(\mathbf{e})$, where ξ is as in (5.16), but with a, b, C, \mathbf{e}_0 and ξ_0 replaced by $a/C_\Omega, b/C_\Omega, C/C_\Omega, \mathbf{e}_{\max}$ and $\xi_{\max}^{3/5}$.

It is easy to see that φ_2 is an increasing, concave curve on $(0, \mathbf{e}_{\max})$, and that $\varphi_2(\mathbf{e}) \searrow 0$ as $\mathbf{e} \searrow 0$. It follows that on $(0, \mathbf{e}_{\max}]$ the curve $\mathcal{E} = \varphi_2(\mathbf{e})$ will stay to the left of that in (5.14); there will exist $\mathbf{e}_{\min} \in (0, \mathbf{e}_{\max})$ for such that $\varphi_2(\mathbf{e}_{\min}) = \mathcal{E}_{\min}$ and $\varphi_2(\mathbf{e}) > \mathcal{E}_{\min}$ for all $\mathbf{e} \in (\mathbf{e}_{\min}, \mathbf{e}_{\max}]$.

In order to show that the assumption (5.9) is satisfied on $[\mathbf{e}_{\min}, \mathbf{e}_{\max}]$, note that from (5.16), with the constants modified by C_Ω and with arbitrary $\mathbf{e}_0, 0 < \mathbf{e} \leq \mathbf{e}_0$,

$$\xi(\mathbf{e}) \geq \mathbf{e}^a \frac{\xi(\mathbf{e}_0)}{\mathbf{e}_0^a},$$

Thus, if we start above the parabola (5.9), i.e. with $\mathcal{E}_0 = \xi_0^{5/3} > 4\|f\|_2 \mathbf{e}_0^{1/2}/\nu$, and to the left of the curve in (5.14), then the corresponding curve φ_2 will satisfy

$$\nu \mathcal{E} \geq \nu \mathcal{E}_0 \left(\frac{\mathbf{e}}{\mathbf{e}_0} \right)^{\frac{1-\rho}{2C_\Omega}} > 4\|f\|_2 \mathbf{e}_0^{\frac{1}{2}} \left(\frac{\mathbf{e}}{\mathbf{e}_0} \right)^{\frac{1-\rho}{2C_\Omega}} = 4\|f\|_2 \mathbf{e}^{\frac{1}{2}} \left(\frac{\mathbf{e}_0}{\mathbf{e}} \right)^{\frac{1}{2} - \frac{1-\rho}{2C_\Omega}} \geq 4\|f\|_2 \mathbf{e}^{\frac{1}{2}},$$

and consequently, the curve $\mathcal{E} = \varphi_2(\mathbf{e})$ will satisfy (5.9) for $\mathbf{e} \in [0, \mathbf{e}_{\max}]$. Therefore, $\mathcal{E} = \varphi_2(\mathbf{e})$ will be a bounding curve for \mathcal{A}_w for $\mathbf{e} \in [\mathbf{e}_{\min}, \mathbf{e}_{\max}]$.

On $\mathbf{e} \in [0, \mathbf{e}_{\min}]$, the assumption (5.5) does not hold, and thus the construction of bounding curves depends on whether $\nu\lambda(\mu + \psi)\mathcal{E}$ dominates $\|\text{curl } F\|_2 \mathcal{E}^{1/2}$ in (5.4). This potentially would introduce two more cases. However, in the case $\|\text{curl } F\|_2$ is big enough, e.g.

$$(5.19) \quad \|\text{curl } F\|_2 \geq c_2 \varepsilon^{3/4} \frac{\lambda^{5/4} \nu^2}{\mu} (\mu + \|\psi\|_\infty)^{9/4},$$

the condition $\mathcal{E} \leq \mathcal{E}_{\max}$ would yield $\|\text{curl } F\|_2 \mathcal{E}^{1/2}$ as the dominating term, and so instead of (5.8) we will obtain

$$(5.20) \quad \frac{d\mathcal{E}}{dt} \leq \left(\frac{c_2 \lambda^{1/2}}{\varepsilon \nu} - \frac{\nu(1-\rho)}{4\mathbf{e}} \right) \mathcal{E}^2 + 6\|\text{curl } F\|_2 \mathcal{E}^{1/2},$$

which together with (5.18) yields the following equations for the bounding curve on $[0, \mathbf{e}_{\min}]$:

$$(5.21) \quad \frac{d\mathcal{E}}{d\mathbf{e}} = \left(\frac{1-\rho}{2C_\Omega \mathbf{e}} - \frac{2c_2 \lambda^{1/2}}{C_\Omega \varepsilon \nu^2} \right) \mathcal{E} - \frac{12}{\nu C_\Omega} \|\text{curl } F\|_2 \mathcal{E}^{-1/2}$$

$$(5.22) \quad \mathcal{E}(\mathbf{e}_{\min}) = \varphi_2(\mathbf{e}_{\min}) = \mathcal{E}_{\min}.$$

Solving this Bernoulli-type equation we obtain

$$x(\mathbf{e}) = x_0 \left(\frac{\mathbf{e}}{\mathbf{e}_{\min}} \right)^\alpha \exp(\beta(\mathbf{e}_{\min} - \mathbf{e})) + \gamma \int_{\mathbf{e}}^{\mathbf{e}_{\min}} \left(\frac{\mathbf{e}}{t} \right)^\alpha \exp(\beta(t - \mathbf{e})) dt,$$

$$x = \mathcal{E}^{3/2}, \quad x_0 = (\mathcal{E}(\mathbf{e}_{\min}))^{3/2}, \quad \alpha = \frac{3}{2} \frac{1-\rho}{2C_\Omega}, \quad \beta = \frac{3c_2 \lambda^{1/2}}{C_\Omega \varepsilon \nu^2}, \quad \gamma = \frac{18}{\nu C_\Omega} \|\text{curl } F\|_2.$$

Note that the above equations imply

$$x(\mathbf{e}) \geq x_0 \left(\frac{\mathbf{e}}{\mathbf{e}_{\min}} \right)^\alpha$$

and therefore, since (5.9) is satisfied by the initial condition (5.22), meaning

$$x_0^{2/3} = \mathcal{E}(\mathbf{e}_{\min}) > 4\|f\|_2 \mathbf{e}_{\min}^{1/2} / \nu,$$

we have for $\mathbf{e} \in [0, \mathbf{e}_{\min}]$

$$\mathcal{E} = (x(\mathbf{e}))^{2/3} \geq x_0^{2/3} \left(\frac{\mathbf{e}}{\mathbf{e}_{\min}} \right)^{\frac{2}{3}\alpha} = \frac{x_0^{2/3}}{\mathbf{e}_{\min}^{1/2}} \mathbf{e}^{1/2} \left(\frac{\mathbf{e}_{\min}}{\mathbf{e}} \right)^{\frac{1}{2} - \frac{2}{3}\alpha} \geq 4\|f\|_2 \mathbf{e}^{1/2} / \nu,$$

i.e. the assumption (5.9) holds on $\mathbf{e} \in [0, \mathbf{e}_{\min}]$, which also means that \mathcal{E} will stay to the left of the curve in (5.14). Therefore,

$$\mathcal{E} = \varphi_3(\mathbf{e}) = (x(\mathbf{e}))^{2/3}$$

is a bounding curve for \mathcal{A}_w for $\mathbf{e} \in (0, \mathbf{e}_{\min}]$. It is easy to see that φ_3 is also increasing, concave and approaches zero as $\mathbf{e} \searrow 0$. In fact,

$$(5.23) \quad \varphi_3(\mathbf{e}) = \mathcal{O} \left(\mathbf{e}^{\frac{1-\rho}{2c_\Omega}} \right) \quad \text{as } \mathbf{e} \searrow 0.$$

We denote the complete bounding curve by

$$\varphi(\mathbf{e}) = \begin{cases} \varphi_1(\mathbf{e}), & \mathbf{e} \in [\mathbf{e}_{\max}, \mathbf{e}_0] \\ \varphi_2(\mathbf{e}), & \mathbf{e} \in [\mathbf{e}_{\min}, \mathbf{e}_{\max}] \\ \varphi_3(\mathbf{e}), & \mathbf{e} \in (0, \mathbf{e}_{\min}) . \end{cases}$$

Since by Poincaré inequality $\lambda_0 \mathbf{e} \leq E$, and by [6] $E \leq c_\Omega \mathcal{E}$, we have the following bounding region for \mathcal{A}_w in $(\mathbf{e}, \mathcal{E})$ -plane:

$$\underline{\lambda} \mathbf{e} \leq \mathcal{E} \leq \phi(\mathbf{e}).$$

with $\underline{\lambda} = \lambda_0 / c_\Omega$.

Numerical solutions of the bounding curve φ are plotted in Figure 2(b). One is made by using a 4th order Runge-Kutta method to solve the ODE, the other two by truncating the series approximation for the incomplete gamma function. Though the Grashof number is quite small ($G = 2$), the maximum value \mathcal{E}_{\max} is at least $\mathcal{O}(10^{35})$. Rigorous upper and lower bounds for \mathcal{E}_{\max} in the next section confirm the dramatic rise in this bounding curve.

In particular, estimates of Section 6 show that as the Grashof number grows, $\mathcal{E}_{\max} \sim \exp(c_3 G^2)$, $\mathbf{e}_a \sim \mathbf{e}_{\max} \sim G^0$, and therefore, we can deduce from (5.16) that $\mathbf{e}_{\min} \sim \exp(-c_4 G^2)$, for appropriate G -independent constants c_3, c_4 . Thus as $G \rightarrow \infty$, the possible big values for enstrophy will be constrained in a narrow (compared to G) strip of energy values located in the proximity of $\mathbf{e} = 0$.

6. ESTIMATES FOR THE MAXIMUM VALUE OF $\mathcal{E} = \varphi(\mathbf{e})$

For simplicity we examine the case $\nu = \lambda = 1$, so that the bounding curve $\mathcal{E} = \varphi_1(\mathbf{e})$ in the critical case is the solution to

$$(6.1) \quad \begin{aligned} \frac{d\mathcal{E}}{d\mathbf{e}} &= - \left(\frac{2c_2}{\varepsilon} - \frac{1-\rho}{2\mathbf{e}} \right) \mathcal{E} - \frac{12c_2\mu}{\varepsilon^{3/5}} \mathcal{E}^{2/5}, \\ \mathcal{E}(\mathbf{e}_0) &= \mathcal{E}_0 = 4\|f\|_2 \mathbf{e}_0^{1/2} = 4G^2. \end{aligned}$$

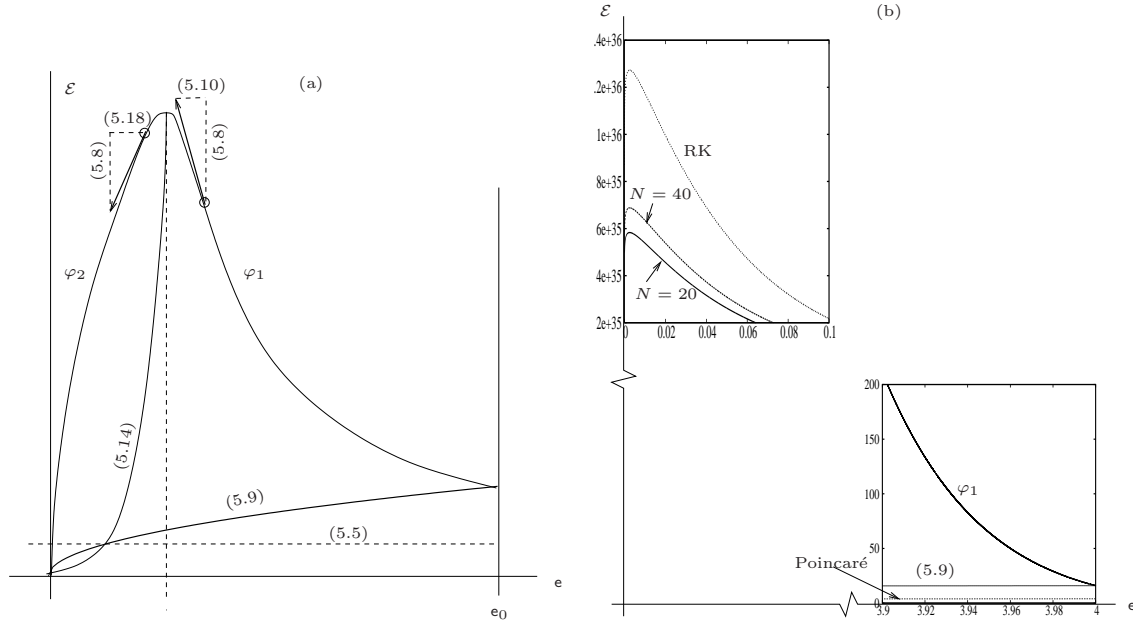


FIGURE 2. (a) Schematic plot indicating which bounds on time derivatives are used to determine the ODEs for φ_1 and φ_2 , (b) Numerically generated bounding curve for $\nu = \lambda = \mu = 1$, $\varepsilon = .2$, $\delta = .5$, $c_2 = G = 2$, by Runge-Kutta (RK) and by truncating the series approximation for the incomplete gamma function to N terms. Estimates for \mathcal{E}_{\max} are in Section 6.

6.1. A lower bound:

Clearly,

$$\frac{d\mathcal{E}}{de} \leq - \left(\frac{2c_2}{\varepsilon} - \frac{1-\rho}{2e} \right) \mathcal{E}.$$

Therefore, on $[e_{\max}, e_0]$ the curve $\mathcal{E} = \varphi(e)$ lies above the solution to

$$(6.2) \quad \begin{aligned} \frac{d\tilde{\mathcal{E}}}{de} &= - \left(\frac{2c_2}{\varepsilon} - \frac{1-\rho}{2e} \right) \tilde{\mathcal{E}}, \\ e_0 &= G^2, \quad \mathcal{E}(e_0) = \mathcal{E}_0 = 4G^2, \end{aligned}$$

which is

$$\tilde{\mathcal{E}}(e) = \mathcal{E}_0 \left(\frac{e}{e_0} \right)^{\frac{1-\rho}{2}} \exp \left(\frac{2c_2}{\varepsilon} (e_0 - e) \right) = 4G^{1+\rho} e^{\frac{1-\rho}{2}} \exp \left(\frac{2c_2}{\varepsilon} (G^2 - e) \right)$$

It is immediate from the ODE in (6.2) that the maximum for $\tilde{\mathcal{E}}$ is achieved when

$$e = e_{\text{crit}} = \frac{\varepsilon(1-\rho)}{4c_2},$$

and therefore the maximal value of the bounding curve $\mathcal{E} = \varphi(e)$ satisfies:

$$(6.3) \quad \mathcal{E}_{\max} \geq 4G^{1+\rho} e_{\text{crit}}^{\frac{1-\rho}{2}} \exp \left(\frac{2c_2}{\varepsilon} (G^2 - e_{\text{crit}}) \right).$$

6.2. An upper bound:

Looking back at the original equations (6.1), we notice that if for $\eta > 0$

$$(6.4) \quad \frac{\eta}{\varepsilon} \mathcal{E} \geq \frac{12\mu}{\varepsilon^{3/5}} \mathcal{E}^{2/5}, \quad \text{or, equivalently} \quad \eta \geq \frac{12\mu}{\varepsilon^{2/5} \mathcal{E}^{3/5}},$$

then

$$\frac{d\mathcal{E}}{de} \geq - \left(\frac{2c_2}{\varepsilon} - \frac{1-\rho}{2e} \right) \mathcal{E} - \frac{\eta c_2}{\varepsilon} \mathcal{E} = - \left(\frac{(2+\eta)c_2}{\varepsilon} - \frac{1-\rho}{2e} \right) \mathcal{E}.$$

Note if (6.4) holds for $\mathcal{E} = \mathcal{E}_0$, then it holds for the bounding curve $\mathcal{E} = \phi(e)$ over $e \in [e_{\max}, e_0]$. Thus, for η big enough so that (6.4) holds at $\mathcal{E} = \mathcal{E}_0$, on the interval $[e_{\max}, e_0]$ the bounding curve $\mathcal{E} = \varphi(e)$ will lie below the solution to the following initial value problem:

$$(6.5) \quad \begin{aligned} \frac{d\tilde{\mathcal{E}}}{de} &= - \left(\frac{(2+\eta)c_2}{\varepsilon} - \frac{1-\rho}{2e} \right) \tilde{\mathcal{E}}, \\ e_0 &= G^2, \quad \tilde{\mathcal{E}}(e_0) = \mathcal{E}_0 = 4G^2. \end{aligned}$$

Obviously, this is exactly (6.2) with $2c_2$ replaced by $(2+\eta)c_2$. Therefore,

$$(6.6) \quad \mathcal{E}_{\max} \leq 4G^{1+\rho} \bar{e}_{\text{crit}}^{\frac{1-\rho}{2}} \exp \left(\frac{(2+\eta)c_2}{\varepsilon} (G^2 - \bar{e}_{\text{crit}}) \right),$$

where

$$\bar{e}_{\text{crit}} = \frac{\varepsilon(1-\rho)}{2(2+\eta)c_2}.$$

Note that $\bar{e}_{\text{crit}} \leq e_{\max} \leq e_{\text{crit}}$, so $e_{\max} \sim \varepsilon$.

Taking $\varepsilon = .2$, $\mu = 1$, $G = c_2 = 2$ in (6.4) we can choose $\eta = 4.33$ to evaluate the expressions in (6.3) and (6.6) and find that

$$5.83 \cdot 10^{35} \leq \mathcal{E}_{\max} \leq 9.13 \cdot 10^{110},$$

which is consistent with the plot in Figure 2(b). Naturally, since G was chosen so small, the upper bound on E_{\max} is much less sharp than the lower bound. We can make the upper bound sharper if we set $\tilde{\mathcal{E}}(e_0) = 39311.12 \gg 4G^2$ in (6.5). Then we can choose $\eta = 0.04$ resulting in the upper bound $E_{\max} \leq 6.99 \cdot 10^{39}$, which is much closer to the lower bound. Note that as G increases, so does \mathcal{E}_0 , and thus the smaller we may take η to sharpen the upper bound.

7. THE SUB-CRITICAL CASE $1/2 < r \leq 1$

Instead of (5.2) we have

$$(7.1) \quad \int_{\Omega} |\mathcal{K}_{222}(x)| dx \leq c\lambda^{r/2} \int_{\Omega} |\omega(x)|^2 \left(\int_{\Omega} \frac{|\omega(y)|}{|x-y|^{3-r}} dy \right) dx$$

$$(7.2) \quad \leq c\lambda^{r/2} \|\omega\|_{8/3}^2 \|h * |\omega|\|_4,$$

where

$$h(x) = \frac{1}{|x|^{3-r}}.$$

To estimate the convolution, we apply the Hölder inequality for convolutions according to

$$1 + \frac{1}{4} = \frac{1}{p} + \frac{1}{q} \quad \text{where} \quad p = \frac{3}{3-r}, q = \frac{12}{3+4r}$$

followed by interpolation to obtain

$$\|h * |\omega|\|_4 \leq c \|h\|_{p,w} \|\omega\|_q \leq c \|\omega\|_q \leq c \|\omega\|_2^{\frac{1+4r}{4}} \|\nabla\omega\|_2^{\frac{3-4r}{4}}.$$

Using this and the interpolation estimate

$$\|\omega\|_{8/3}^2 \leq c \|\omega\|_2^{5/4} \|\nabla\omega\|_2^{3/4}$$

into (7.1), we have

$$\begin{aligned} \int_{\Omega} |\mathcal{K}_{222}(x)| \, dx &\leq c \lambda^{r/2} \|\omega\|_2^{\frac{3+2r}{2}} \|\nabla\omega\|_2^{\frac{3-2r}{2}} \\ &\leq \varepsilon \nu \|\nabla\omega\|_2^2 + c \left(\frac{\lambda^{2r}}{(\varepsilon\nu)^{3-2r}} \right)^{\frac{1}{1+2r}} \|\omega\|_2^{\frac{6+4r}{1+2r}}. \end{aligned}$$

This gives a bound just as in (5.4), except that

$$\frac{\lambda^{1/2}}{\varepsilon\nu} \mathcal{E} \quad \text{is replaced by} \quad \left(\frac{\lambda^{2r}}{(\varepsilon\nu)^{3-2r}} \right)^{\frac{1}{1+2r}} \mathcal{E}^{\frac{2}{1+2r}}.$$

Thus, under a threshold condition

$$(7.3) \quad \mathcal{E} \geq \underline{\mathcal{E}},$$

where $\underline{\mathcal{E}}$ is defined similarly to \mathcal{E}_{\min} in (5.5) so that the summand with the $\frac{2}{1+2r}$ power dominates the others, we have

$$(7.4) \quad \frac{d\mathcal{E}}{dt} \leq -\frac{\nu(1-\rho)}{4e} \mathcal{E}^2 + \nu \frac{C}{2} \mathcal{E}^{\frac{3+2r}{1+2r}}$$

where

$$C = \frac{2}{\nu} 6c \left(\frac{\lambda^{2r}}{(\varepsilon\nu)^{3-2r}} \right)^{\frac{1}{1+2r}}.$$

We then combine (7.5) with (5.10) to find a bounding curve solving

$$(7.5) \quad \frac{d\mathcal{E}}{de} = \frac{1-\rho}{2e} \mathcal{E} - C \mathcal{E}^{\frac{2}{1+2r}}$$

over the interval $[\bar{e}, e_0]$ where (7.4) is nonnegative. The solution to (7.5) is

$$(7.6) \quad \mathcal{E} = \phi_1(e) = \left\{ \left(\frac{e}{e_0} \right)^{\alpha\sigma} \mathcal{E}_0^\sigma + \frac{\sigma C}{1-\alpha\sigma} \left[\frac{e^{\alpha\sigma}}{e_0^{\alpha\sigma-1}} - e \right] \right\}^{1/\sigma},$$

where

$$\sigma = \frac{2r-1}{1+2r}, \quad \text{and} \quad \alpha = \frac{1-\rho}{2}.$$

From (7.5), we have that the maximum value, $\bar{\mathcal{E}} = \phi_1(\bar{e})$ is achieved where the bounding curve (7.6) intersects the curve $\alpha\mathcal{E}^\sigma = Ce$. An elementary calculation gives, for appropriate G -independent constants C_1 and C_2 ,

$$\bar{\mathcal{E}} = [C_1(G^2)^{\sigma-\alpha\sigma} + C_2(G^2)^{1-\alpha\sigma}]^{\frac{1}{\sigma(1-\alpha\sigma)}} = \mathcal{O}(G^{2/\sigma})$$

as $G \rightarrow \infty$.

For $e < \bar{e}$, as long as (7.3) and (5.9) hold, we combine (7.4) with (5.18) to obtain a bounding curve $\mathcal{E} = \phi_2(e)$ where ϕ_2 is the same as ϕ in (7.6) except α , C , e_0 and \mathcal{E}_0 are replaced by α/C_Ω , C/C_Ω , \bar{e} and $\bar{\mathcal{E}}$. As in Section 5, we can show that ϕ_2 is an increasing concave curve that converges to zero at the origin and stays above

the parabola $\mathcal{E} = 4\|f\|_2 e^{1/2}/\nu$ over the interval $[0, \bar{e}]$. Therefore ϕ_2 will intersect the line $\mathcal{E} = \underline{\mathcal{E}}$ at some point $\underline{e} \in (0, \bar{e})$, and so

$$\mathcal{E} = \phi_2(e)$$

is a bounding curve for \mathcal{A}_w on $[\underline{e}, \bar{e}]$.

The bounding curve for $0 < e < \underline{e}$ is obtained analogously to ϕ_3 in Section 5. In fact if $\mathcal{E} \leq \underline{\mathcal{E}}$ and $\|\text{curl } F\|_2$ is bigger than an appropriate Grashof-independent threshold similar to (5.19), then the term $\|\text{curl } F\|_2 \mathcal{E}^{1/2}$ will dominate, resulting in the following equivalent of (5.21-5.22):

$$(7.7) \quad \frac{d\mathcal{E}}{de} = \frac{1-\rho}{2C_\Omega e} \mathcal{E} - \frac{12}{C_\Omega} \|\text{curl } F\|_2 \mathcal{E}^{-1/2}$$

$$(7.8) \quad \mathcal{E}(\underline{e}) = \phi_2(\underline{e}).$$

This yields the curve

$$(7.9) \quad \mathcal{E} = \phi_3(e) := \left\{ \left(\frac{e}{\underline{e}} \right)^{3\beta/2} \underline{\mathcal{E}}^{3/2} + \frac{36\|\text{curl } F\|_2}{C_\Omega(2-3\beta)} \left[\frac{e^{3\beta/2}}{\underline{e}^{3\beta/2-1}} - e \right] \right\}^{2/3}$$

with $\beta = (1-\rho)/(2C_\Omega)$. As in Section 5, $\phi_3(e)$ is increasing on $(0, \underline{e}]$, convergent to zero at 0, and is above the parabola $\mathcal{E} = 4\|f\|_2 e^{1/2}/\nu$. Also,

$$(7.10) \quad \phi_3(e) = \mathcal{O}\left(e^{\frac{1-\rho}{2C_\Omega}}\right) \quad \text{as } e \searrow 0,$$

i.e. *the same rate* as in critical case – see (5.23).

Thus we obtain the following bounding region for \mathcal{A}_w in (e, \mathcal{E}) -plane:

$$\underline{\Delta} e \leq \mathcal{E} \leq \phi(e) := \begin{cases} \phi_1(e), & e \in [\bar{e}, e_0] \\ \phi_2(e), & e \in [\underline{e}, \bar{e}] \\ \phi_3(e), & e \in (0, \underline{e}) . \end{cases}$$

These bounds are illustrated in Figure 3.

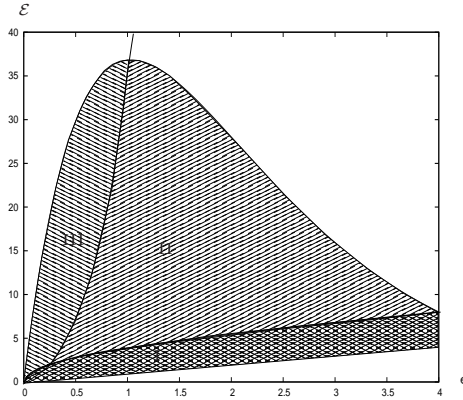


FIGURE 3. Bounding curves for subcritical case, $r = .51$, $G = 2$, $C = 1$. Region I is recurrent. In region III the enstrophy is always decreasing, while in regions II and III the energy is always decreasing.

8. BOUNDS FROM SCALING-INVARIANT REGULARITY CONDITION

A natural question to pose at this point—for the sake of comparison—is what are the effects of the classical, analytical *scaling-invariant* regularity criteria on the vorticity magnitude on the dynamics considered in the energy-enstrophy plane. As an illustration, we present the case of the small- $L^{\frac{3}{2}}$ spatial integrability condition,

$$\sup_{t \in (0, T)} \|\omega(t)\|_{\frac{3}{2}} \leq \epsilon_0,$$

for a sufficiently small constant ϵ_0 .

In this case, the estimate on the vortex-stretching term reads as follows.

$$\begin{aligned} \int_{\Omega} |\omega \cdot \nabla u \cdot \omega| dx &\leq \|\omega\|_{\frac{3}{2}} \|\nabla u\|_6 \|\omega\|_6 \\ &\leq C_{\Omega} \|\omega\|_{\frac{3}{2}} \|\omega\|_6^2 \leq c_{\Omega} \|\omega\|_{\frac{3}{2}} \left(\|\nabla \omega\|_2^2 + k_{\Omega} \|\omega\|_2^2 \right) \\ &\leq \epsilon_0 c_{\Omega} \left(\|\nabla \omega\|_2^2 + k_{\Omega} \|\omega\|_2^2 \right) \\ &\leq \epsilon_0 c'_{\Omega} \nu \left(\|\nabla \omega\|_2^2 + \lambda \|\omega\|_2^2 \right). \end{aligned}$$

Using this along with (5.1), (5.7) yields

$$\frac{d\mathcal{E}}{dt} \leq -\frac{\nu}{4}(1 - \epsilon_0 c'_{\Omega} - \delta) \frac{\mathcal{E}^2}{e} + 2\nu\lambda(\psi + \epsilon_0 c'_{\Omega})\mathcal{E} + 2\|\operatorname{curl} F\|_2 \mathcal{E}^{1/2}.$$

Now assume

$$\mathcal{E} \geq \left(\frac{\|\operatorname{curl} F\|_2}{\nu\lambda(\psi + \epsilon_0 c'_{\Omega})} \right)^2,$$

so that

$$\frac{d\mathcal{E}}{dt} \leq -\frac{\nu\alpha}{2e} \mathcal{E}^2 + \frac{\nu\beta}{2} \mathcal{E}$$

where if we take ϵ_0, δ small enough

$$0 < \alpha = \frac{1}{2}(1 - \epsilon_0 c'_{\Omega} - \delta) < 1 \quad \beta = 8\lambda(\psi + \epsilon_0 c'_{\Omega}).$$

We combine with (5.10), and thus consider

$$\frac{d\mathcal{E}}{de} = \frac{\alpha}{e} \mathcal{E} - \beta, \quad \mathcal{E}(e_0) = \mathcal{E}_0$$

whose solution is given by

$$\mathcal{E} = \left(\frac{\mathcal{E}_0}{e_0^{\alpha}} + \frac{\beta e_0^{1-\alpha}}{1-\alpha} \right) e^{\alpha} - \frac{\beta}{1-\alpha} e.$$

This curve provides a bound as long as $d\mathcal{E}/de < 0$, i.e., for

$$e_{\max} = \left[\frac{\alpha(1-\alpha)}{\beta} \left(\frac{\mathcal{E}_0}{e_0^{\alpha}} + \frac{\beta e_0^{1-\alpha}}{1-\alpha} \right) \right]^{\frac{1}{1-\alpha}} < e \leq e_0,$$

which gives a maximal value of

$$\mathcal{E}_{\max} = \mathcal{E}(e_{\max}) \sim G^{4-2\alpha}$$

(ignoring the dependence on ν, λ).

This is somewhat unexpected. With respect to the scaling associated with the 3D NSE, the $L^{\frac{3}{2}}$ -condition is scaling-invariant, while the $\frac{1}{2}$ -Hölder coherence condition exhibits sub-critical scaling. Hence, from this point of view, the scaling-invariant condition is a weaker condition. In contrast, when considering dynamics of the solutions, at least within the realm of bounding curves in the energy, enstrophy plane, the $\frac{1}{2}$ -Hölder coherence condition appears to be much weaker as it allows for *qualitatively* higher maximum values of the enstrophy: exponential *vs.* algebraic (in Grashof). Incidentally, this is philosophically consistent with another very recent result illustrating discrepancies between the scaling and dynamical properties of solutions to the 3D NSE [5].

To compare the $L^{\frac{3}{2}}$ scaling-invariant case to the r -Hölder coherence assumption in the case $\frac{1}{2} < r \leq 1$, in terms of G , we set

$$\frac{4r+2}{2r-1} = 4 - 2\alpha = 3 + \epsilon_0 c'_\Omega + \delta, \quad \text{i.e.,} \quad r = \frac{\epsilon_0 c'_\Omega + \delta + 5}{2(\epsilon_0 c'_\Omega + \delta) + 2}$$

and find that

$$0 < \epsilon_0 c'_\Omega + \delta < 1 \implies 3/2 < r < 5/2.$$

Since

$$\frac{4r+2}{2r-1} > 4 - 2\alpha \quad \text{for} \quad 1/2 < r < 3/2,$$

we conclude that even the stronger $\frac{1}{2} < r \leq 1$ Hölder coherence assumption—in principle—allows for larger values of the maximal enstrophy than the $L^{\frac{3}{2}}$ -integrability condition, and is in this sense a dynamically weaker condition.

REFERENCES

- [1] W. Ashurst, W. Kerstein, R. Kerr, and C. Gibson. Alignment of vorticity and scalar gradient with strain rate in simulated Navier-Stokes turbulence. *Phys. Fluids*, 30:2343, 1987.
- [2] H. Beirão da Veiga. Vorticity and regularity for viscous incompressible flows under the Dirichlet boundary condition. results and related open problems. *J. Math. Fluid Mechanics*, 9:506–516, 2007.
- [3] H. Beirão da Veiga and Luigi C. Berselli. On the regularizing effect of the vorticity direction in incompressible viscous flows. *Differential Integral Equations*, 15(3):345–356, 2002.
- [4] H. Beirão da Veiga and Luigi C. Berselli. Navier-Stokes equations: Green’s matrices, vorticity direction, and regularity up to the boundary. *J. Differential Equations*, 246(2):597–628, 2009.
- [5] Z. Bradshaw and Z. Grujić. Scaling vs. dynamics in the 3D NSE. A vignette. *arXiv:1501.01043v1*, 2015.
- [6] C. H. A. Cheng and S. Shkoller. Solvability and regularity for an elliptic system prescribing the curl, divergence and partial trace of a vector field on Sobolev-class domains. *arXiv:1408.2469v1*, 2014.
- [7] V. Chepyzhov, Titi E. S., and M. Vishik. On the convergence of solutions of the 3d Leray- α model to the trajectory attractor of the 3d Navier-Stokes system. *Discr. & Cont. Dyn. Systems A*, 17(3):481–500, 2007.
- [8] P. Constantin. Geometric statistics in turbulence. *SIAM Rev.*, 36:73–98, 1994.
- [9] P. Constantin and C. Fefferman. Direction of vorticity and the problem of global regularity for the Navier-Stokes equations. *Indiana Univ. Math. J.*, 42:775–789, 1993.
- [10] P. Constantin and C. Foias. *Navier-Stokes equations*. Chicago Lectures in Mathematics. University of Chicago Press, Chicago, IL, 1988.
- [11] R. Dascaliuc, C. Foias, and M. S. Jolly. Relations between energy and enstrophy on the global attractor of the 2-D Navier-Stokes equations. *J. Dynamics Differential Equations*, 17:643–736, 2005.
- [12] R. Dascaliuc, C. Foias, and M. S. Jolly. Estimates on enstrophy, palinstrophy, and invariant measures for 2-D turbulence. *J. Differential Eqns*, 248:792–819, 2010.

- [13] A. Farhat, M. S. Jolly, and E. Lunasin. Enstrophy bounds for the 3D Navier-Stokes- α and Leray- α turbulence models. *Comm. Pure & Appl. Anal.*, 13(5), 2014.
- [14] C. Foias. Statistical study of the Navier-Stokes equations, ii. *Rend. Sem. Mat. Univ. Padova*, 49:9–123, 1973.
- [15] C. Foias and C. Guillopé. On the behavior of solutions of the Navier-Stokes equations lying on invariant manifolds. *J. Differential Eq.*, 61:128–148, 1986.
- [16] C. Foias, M. S. Jolly, O. P. Manley, R. Rosa, and R. Temam. Kolmogorov theory via finite-time averages. *Phys. D*, 212(3-4):245–270, 2005.
- [17] C. Foias, O. P. Manley, R. Rosa, and R. Temam. Estimates for the energy cascade in three-dimensional turbulent flows. *C. R. Acad. Sci. Paris Sér. I Math.*, 333(5):499–504, 2001.
- [18] C. Foias and R. Temam. The connection between the Navier-Stokes equations, dynamical systems, and turbulence theory. In *Directions in partial differential equations (Madison, WI, 1985)*, volume 54 of *Publ. Math. Res. Center Univ. Wisconsin*, pages 55–73. Academic Press, Boston, MA, 1987.
- [19] Z. Grujić. Localization and geometric depletion of vortex-stretching in the 3D NSE. *Comm. Math. Phys.*, 290(3):861–870, 2009.
- [20] Z. Grujić and R. Guberović. Localization of analytic regularity criteria on the vorticity and balance between the vorticity magnitude and coherence of the vorticity direction in the 3D NSE. *Comm. Math. Phys.*, 298(2):407–418, 2010.
- [21] J. Jiménez, A. A. Wray, P. G. Saffman, and Robert S. Rogallo. The structure of intense vorticity in isotropic turbulence. *J. Fluid Mech.*, 255:65–90, 1993.
- [22] A. N. Kolmogorov. The local structure of turbulence in incompressible viscous fluid for very large Reynolds numbers. *Proc. Roy. Soc. London Ser. A*, 434(1890):9–13, 1991. Translated from the Russian by V. Levin, *Turbulence and stochastic processes: Kolmogorov’s ideas 50 years on*.
- [23] R. H. Kraichnan. Inertial ranges in two-dimensional turbulence. *Phys. Fluids*, 10:1417–1423, 1967.
- [24] P. G. Lemarié-Rieusset. *Recent developments in the Navier-Stokes problem*, volume 431 of *Chapman & Hall/CRC Research Notes in Mathematics*. Chapman & Hall/CRC, Boca Raton, FL, 2002.
- [25] L. Lu and Doering C. R. Limits on enstrophy growth for solutions of the three-dimensional Navier-Stokes equations. *Indiana University Mathematics J.*, 57(6):2693–2727, 2008.
- [26] Doering C. R. The 3D Navier-Stokes problem. *Annu. Rev. Fluid Mech.*, 41:109–128, 2009.
- [27] Z.-S. She, E. Jackson, and S. A. Orszag. Structure and dynamics of homogeneous turbulence: models and simulations. *Proc. R. Soc. Lond. A.*, 434:101–124, 1991.
- [28] E. M. Stein. *Singular integrals and differentiability properties of functions*, volume 30 of *Princeton Mathematical Series*. Princeton University Press, Princeton, N.J., 1970.
- [29] R. Temam. *Navier-Stokes Equations: Theory and Numerical Analysis*. AMS Chelsea, third edition, 1984.
- [30] R. Temam. *Infinite-dimensional dynamical systems in mechanics and physics*, volume 68 of *Applied Mathematical Sciences*. Springer-Verlag, New York, second edition, 1997.
- [31] A. Vincent and M. Meneguzzi. The dynamics of vorticity tubes of homogeneous turbulence. *J. Fluid Mech.*, 258(5):245 – 254, 1994.
- [32] M. Vishik, Titi E. S., and V. Chepyzhov. On convergence of trajectory attractors of the 3d Navier-Stokes- α model as α approaches 0. *Matematicheskii Sbornik*, 198(12):3–36, 2007.

¹DEPARTMENT OF MATHEMATICS, OREGON STATE UNIVERSITY, CORVALLIS, OR 97331

²DEPARTMENT OF MATHEMATICS, UNIVERSITY OF VIRGINIA, CHARLOTTESVILLE, VA 22904

³DEPARTMENT OF MATHEMATICS, INDIANA UNIVERSITY, BLOOMINGTON, IN 47405

E-mail address, R. Dascaliuc: dascalir@math.oregonstate.edu

E-mail address, Z. Grujic: zg7c@virginia.edu

E-mail address, M. S. Jolly: msjolly@indiana.edu